

# Electromagnetically induced transparency in a sodium vapour cell

S. Balushev<sup>a</sup>, N. Leinfellner, E.A. Korsunsky, and L. Windholz<sup>b</sup>

Institut für Experimentalphysik, Technische Universität Graz, 8010 Graz, Austria

Received: 17 December 1997 / Accepted: 6 March 1998

**Abstract.** We report on an investigation of electromagnetically induced transparency (EIT) in sodium vapour. In our experiment, sodium atoms are excited on the D<sub>1</sub>-line with laser radiation containing two components with a frequency difference close to that of the two hyperfine ground states of sodium (1.772 GHz). Such an excitation leads to coherent trapping of atomic population in “dark” superpositional states, which dramatically reduces the absorption of light. A frequency transparency window is measured to have a subnatural width, which is a clear indication of coherent population trapping. Dependence of EIT on laser frequencies and intensities, on the magnetic field strength as well as on the temperature of the sodium vapour is studied.

**PACS.** 32.80.-t Photon interactions with atoms – 42.50.-p Quantum optics

## 1 Introduction and theoretical considerations

Electromagnetically induced transparency (EIT) is an effect of reduction (or even cancellation in an ideal case) of light absorption by an atomic medium at particular frequencies near an atomic resonance [1]. The origin of this effect is the destructive quantum interference between light-induced atomic transitions. The combination of coherent light excitation and spontaneous emission quickly puts atoms into a superposition quantum state which is insensitive to laser radiation. Thus, EIT is a technique for the creation of a phase coherent atomic ensemble (“phaseonium” [2]) which may be a basis for new types of optoelectronic devices. Recently, EIT attracted a lot of attention. A major driving force behind these studies is the application of EIT to related topics of high sensitivity magnetometry and gravimetry [3], lasing without population inversion [4], enhancement of non-linear wave-mixing processes [5], correlation of laser phase fluctuations [6] and quantum noise reduction [7].

In the present paper we investigate the EIT effect based on coherent population trapping [8]. The simplest quantum system where coherent population trapping (CPT) is possible is a three-level  $\Lambda$  atom (Fig. 1a). In this system, a specific superposition of two ground states  $|1\rangle$  and  $|2\rangle$  is formed which is completely decoupled from the laser field at the two-photon resonance  $\Delta_1 = \Delta_2$ . The population of the system is optically pumped into this non-coupled state (also called “dark state”)  $|NC\rangle$  and trapped

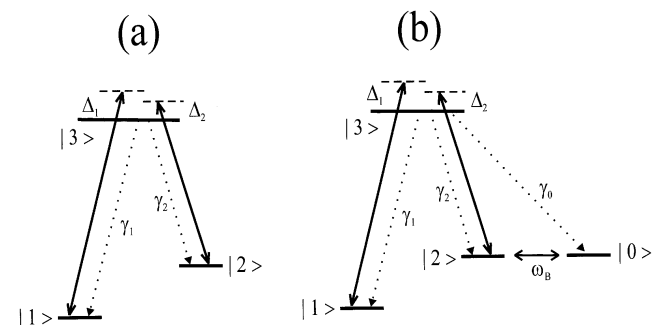


**Fig. 1.** (a) Three-level  $\Lambda$  system. (b) Four-level system:  $\Lambda$  system with additional radiative decay to an external state  $|0\rangle$ . The spontaneous decay rates are denoted by  $\gamma_m$  for  $|3\rangle \rightarrow |m\rangle$  decay channels ( $m = 0, 1, 2$ ), and the detunings are  $\Delta_m$  for  $|m\rangle - |3\rangle$  transitions ( $m = 1, 2$ ).  $\omega_B$  is the Larmor frequency for the population precession between states  $|2\rangle$  and  $|0\rangle$  due to the perpendicular magnetic field.

there. The consequence is a lossfree transmission of the laser light at frequencies corresponding to the two-photon resonance, in contrast to the exponential decay (Beer’s law) at other frequencies [9].

However, it is very difficult to find a pure  $\Lambda$  scheme in real atomic systems. For example, laser excitation of alkali atoms involves tens of Zeeman sublevels. Usually, the  $\Lambda$ -type EIT experiments with alkali atoms are performed by use of two lasers. When their radiations are orthogonally linearly polarized then the interaction scheme can be effectively approximated by the three-level  $\Lambda$  system [10,11]. We use in our experiment two optical

<sup>a</sup> Permanent address: Technical University of Sofia, Institute of Applied Physics, 1756 Sofia, Bulgaria

<sup>b</sup> e-mail: windholz@fexphds01.tu-graz.ac.at

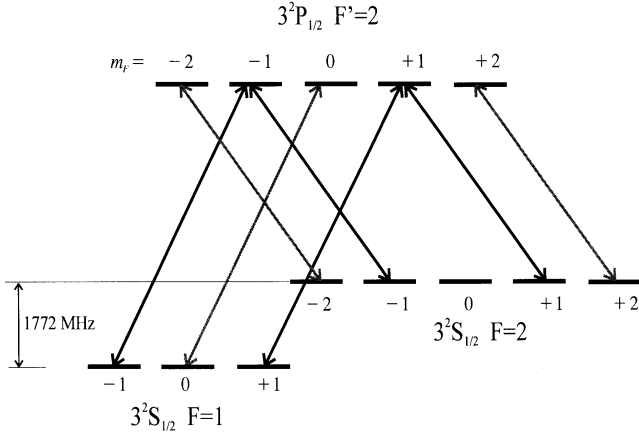


**Fig. 2.** The relevant structure of the  $3^2S_{1/2}$  and  $3^2P_{1/2}$  levels of sodium. The  $m_F$  quantum number denotes the projection of the atomic angular momentum  $F$  on the axis parallel to the laser polarization ( $z$ -axis).

frequencies derived from one laser with an electro-optical modulator (EOM). This method has an additional advantage of perfect amplitude and phase correlation of both laser frequencies. Therefore, the EIT frequency resolution is not limited by the bandwidth of the laser. However, the two harmonics produced by the EOM are spatially overlapping and equally (linear) polarized. Their frequency difference matches the hyperfine splitting of the  $3^2S_{1/2}$  ground state of Na so that they are tuned on the  $F = 1 \leftrightarrow F' = 2$  ( $3^2P_{1/2}$ ) and  $F = 2 \leftrightarrow F' = 2$  ( $3^2P_{1/2}$ ) transitions, respectively (for zero-velocity atoms). In this configuration, two three-level  $\Lambda$  schemes:  $F = 1 \leftrightarrow F' = 2 \leftrightarrow F = 2$  ( $m_F = +1$  and  $m_F = -1$ ) are formed, and the Zeeman sublevel  $F = 2$ ,  $m_F = 0$  is not excited by the laser radiation (Fig. 2). The  $\Lambda$  systems are responsible for the creation of CPT, and the state  $F = 2$ ,  $m_F = 0$  serves as a sink in the regular optical pumping process. In such a situation (sometimes referred to as coherent optical pumping [12]), a fraction of the atomic population is trapped in the CPT states and the rest is pumped into the state  $F = 2$ ,  $m_F = 0$ . We model this process by using a four-level system consisting of the  $\Lambda$  system with an upper state decaying not only to the states  $|1\rangle$  and  $|2\rangle$  but also into the state  $|0\rangle$  (Fig. 1b) [12, 13].

We consider an interaction of  $\Lambda$  atoms or four-level atoms (Fig. 1) with the bichromatic linearly polarized laser field propagating along the  $x$ -axis

$$\mathbf{E} = E_1 \mathbf{e}_z \cos(\omega_1 t - k_1 x) + E_2 \mathbf{e}_z \cos(\omega_2 t - k_2 x), \quad (1)$$

where  $\mathbf{e}_z$  is the polarization unit vector. We assume that the wave having an amplitude  $E_1$  and frequency  $\omega_1$  excites the  $|1\rangle$ — $|3\rangle$  transition only, whereas the wave having  $E_2$  and  $\omega_2$  excites the  $|2\rangle$ — $|3\rangle$  transition only. Transmission of the light fields through the medium is governed by the Maxwell wave equations. For slowly varying amplitudes and in the steady state, they are reduced to following

equations (see, *e.g.* Ref. [14])

$$\frac{\partial g_m}{\partial \zeta} = -\frac{\gamma_m}{\gamma} \text{Im} \langle \rho_{3m} \rangle, \quad (m = 1, 2) \quad (2)$$

for dimensionless field amplitudes  $g_m = \mathbf{e}_z \cdot \mathbf{d}_{3m} E_m / 2\hbar\gamma$ . Here  $\mathbf{d}_{3m}$  are the dipole moments of the  $|m\rangle$ — $|3\rangle$  transitions ( $m = 1, 2$ ), and  $\gamma$  is the total spontaneous decay rate of the excited state  $|3\rangle$ .  $\langle \rho_{3m} \rangle$  are the off-diagonal elements  $\langle 3 | \hat{\rho} | m \rangle$  of the atomic density matrix  $\hat{\rho}$  averaged over the velocity distribution  $M(v)$ :  $\langle \rho_{3m} \rangle = \int_{-\infty}^{+\infty} \rho_{3m}(v) M(v) dv$ . The dimensionless optical length  $\zeta$  is determined as  $\zeta = (3\pi c^2 N / 4\omega_1^2) x$  with  $N$  being the atomic vapour density.

Absorption characteristics of the atomic medium are determined by the imaginary part of the susceptibility which is proportional to the stationary value of the imaginary part of the optical coherence  $\rho_{3m}$  for the waves resonant to  $|m\rangle$ — $|3\rangle$  transitions. The absorption coefficient is zero at the two-photon resonance for the  $\Lambda$  atom (dotted curve in Fig. 3a) which results in the transparency of the medium. In the case of coherent optical pumping (four-level system in Fig. 1b), the stationary value of optical coherences is zero for any laser detuning, hence the absorption is due to the transient regime of the pumping only. Therefore, we calculate the temporal dependence of the density matrix elements, and substitute into equation (2) not the stationary, but averaged over the interaction time values of optical coherences  $\rho_{3m}$ . Such an approach accounts automatically for the finite time spent by atoms in the laser light. One can see that the light absorption is generally weaker than in an atomic  $\Lambda$  medium (dashed curve in Fig. 3a). Also, the absorption is not completely cancelled for the two-photon resonance frequencies  $\Delta_1 = \Delta_2$ . As a result, the contrast of the absorption spectra is much smaller for the case of coherent optical pumping than for the case of  $\Lambda$ -atoms. The numerical solution of the Maxwell equations (2) is shown in Figure 3b for the cases corresponding to absorption coefficients presented in Figure 3a. Furthermore we note, that the width of the CPT resonance is proportional to the laser light intensity [8]. Therefore, as the light intensity weakens during the propagation through the medium, the transparency window (the narrow frequency range of the light absorption reduction) decreases with increasing the optical length [9].

The situation in the real laser-atom interaction scheme essentially depends on the presence of a magnetic field too. The components of the external magnetic field, perpendicular to the  $z$ -axis, would induce transitions between Zeeman sublevels of one hyperfine state. We model this coupling in the frame of our four-level system by a precession of the population between states  $|2\rangle$  and  $|0\rangle$  (between  $|F = 2, m_F = 1\rangle$  and  $|F = 2, m_F = 0\rangle$ ) with a Larmor frequency  $\omega_B = g_F \mu_B B / \hbar$  ( $g_F = 1/2$  is the Landé factor of the ground state [15]). With this notation we get  $\omega_B = 0.07\gamma$  for  $B = 1$  G ( $\gamma = 6.3 \times 10^7$  s $^{-1}$  for Na). The effect of the perpendicular magnetic field is twofold. Firstly, since the state  $|0\rangle$  is not a perfect trap state anymore, the absorption increases for all detunings. At the same time, transitions from the state  $|2\rangle$  to the state  $|0\rangle$  lead to a decay of the superposition dark state  $|NC\rangle$ . Therefore,

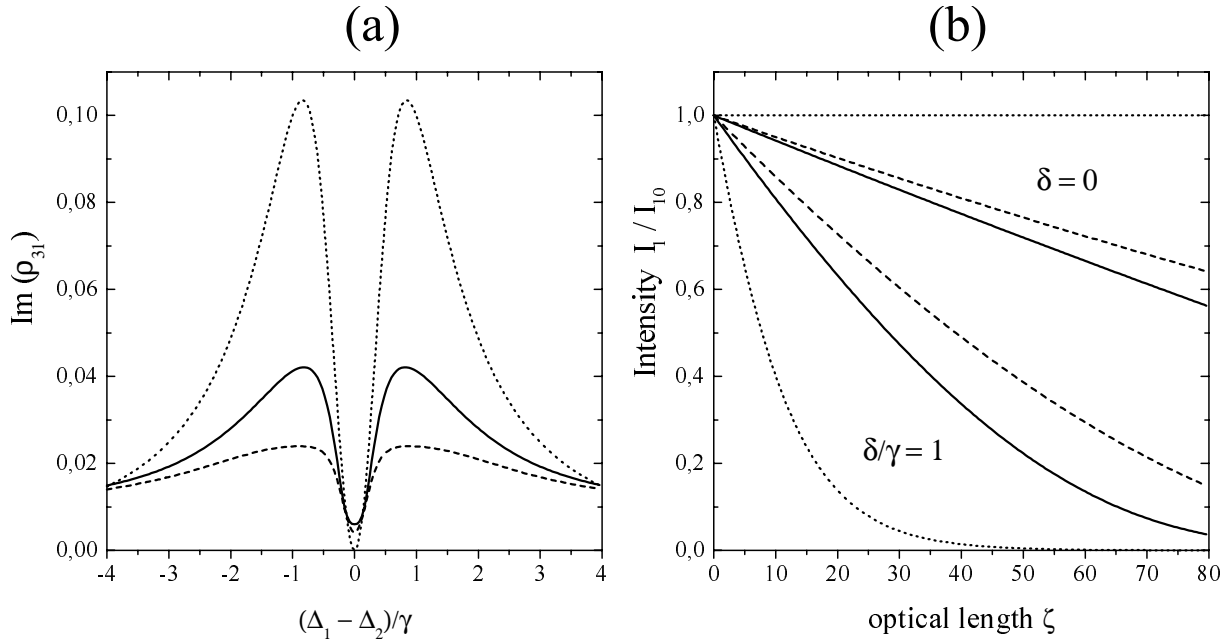


**Fig. 3.** (a) Dependence of the absorption coefficient (which is proportional to  $\text{Im}(\rho_{31})$ ) for the field  $E_1$  on the “Raman” detuning  $\delta = \Delta_1 - \Delta_2$ . (b) Dependence of the intensity of the laser wave  $\omega_1$  (normalized to the input intensity) on the optical length  $\zeta$  for the exact two-photon resonance  $\delta = 0$  (upper group of curves) and out of two-photon resonance  $\delta/\gamma = 1$  (lower group of curves). For both figures, dotted curves correspond to the three-level  $\Lambda$  system,  $\gamma_1 = \gamma_2 = 0.5\gamma$ , input Rabi frequencies  $g_{10} = g_{20} = 0.5$ . Dashed and solid curves correspond to the four-level system (Fig. 1b) with  $\gamma_1 = 0.5\gamma$ ,  $\gamma_2 = 0.3\gamma$ ,  $\gamma_0 = 0.2\gamma$ ,  $g_{10} = g_{20} = 0.5$ , interaction time  $t = 100\gamma^{-1}$ , and Larmor frequency  $\omega_B = 0$  (dashed curves) and  $\omega_B/\gamma = 0.07$  (solid curves).

the transparency of the medium at two-photon resonance decreases further. The existence of CPT in such a system requires that the pumping rate into  $|NC\rangle$  should exceed its decay. This gives the condition [13]

$$(g_1^2 + g_2^2)\gamma \gg \omega_B. \quad (3)$$

Since the light intensity weakens during the propagation through the medium (solid curves in Fig. 3b), this condition may be violated after a sufficiently large optical length even if the initial intensity ( $g_{10}^2 + g_{20}^2$ ) were high enough. The transmitted intensity decreases linearly with the optical length with the slope proportional to  $\omega_B$ :  $g_m^2 = g_{m0}^2 - \alpha(\omega_B/\gamma)\zeta$ . Therefore the condition equation (3) can be expressed in terms of the optical length as

$$\zeta\omega_B \ll (g_{10}^2 + g_{20}^2)\gamma. \quad (4)$$

These considerations demonstrate the importance of a magnetic shielding for the observation of EIT.

## 2 Experiment

The experimental setup is shown in Figure 4. The CW dye laser, using Rhodamine 6G and driven by an  $\text{Ar}^+$ -laser provides a single frequency, coherent, linearly polarized light for the experiment. The frequency of the laser light is tuned to the  $D_1$  transition ( $3^2S_{1/2} - 3^2P_{1/2}$ ) of atomic sodium. An EOM, modulated by a precise frequency generator (modulation frequency  $f_g$ ) was used to

produce a pair of two side bands having the same frequency difference as the hyperfine splitting of the two ground levels  $3^2S_{1/2}, F = 1$  and  $3^2S_{1/2}, F = 2$  (1772 MHz without magnetic field). By detuning the EOM from the exact match of the splitting one can either fulfill or violate the two photon resonance condition necessary for the establishment of CPT. The output of the EOM still contains, apart from those first-order side bands, the zeroth order (carrier frequency) component and the second order side bands. The light passes an electronically controlled Fabry-Perot interferometer (FPI) which suppresses the zeroth order and second order side bands. This is necessary because the carrier frequency is tuned exactly in the middle of the (Doppler broadened)  $3^2S_{1/2}, F = 1 - 3^2P_{1/2}$  and  $3^2S_{1/2}, F = 2 - 3^2P_{1/2}$  transitions. Therefore, it would be absorbed quite weakly and would give an additional background to the signal. Another, minor effect of the zeroth order would be that, for the atoms which have already been prepared in the CPT state by sidebands modes, two velocity groups of these atoms (Doppler shifted by  $\pm 886$  MHz) would be excited by the central mode and jump out of the CPT state. Thus, we could not observe the EIT effect without using the FPI mode filter.

In order to avoid light reflection back into the laser due to the FPI, a combination of two quarter-wave length plates (QWP) and a polarizing beam splitter cube (PBS) is used. After the second quarter-wave plate, the light is again linearly polarized. A lens (L) provides focusing of the beam within the cell. The waist of the focused beam of 0.53 mm ( $1/e$ -width of Gaussian transversal laser profile)

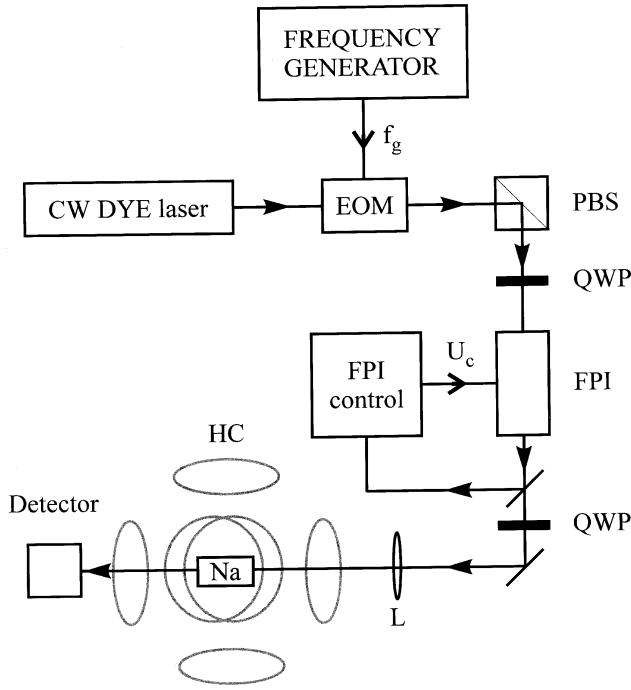


**Fig. 4.** Scheme of the experimental setup. EOM, electro optical modulator; PBS, polarizing beam splitter cube; QWP, quarter-wave plates; FPI, Fabry-Perot interferometer; FPI control, acousto-mechanical re-adjustment of FPI, self tuned to the highest possible output amplitude; L, focusing lens ( $f = 500$  mm); HC, arrangement of three perpendicular pairs of Helmholtz coils; Na, vacuum cell filled with sodium; Detector, photo diode with data acquisition system.

spreads over the whole cell. Therefore, one can consider such a beam as nearly parallel within the probe region. After passing the cell, the light intensity was detected by a photodiode and then recorded by a computer controlled data acquisition system. The cell itself is 10 cm long and 26 mm in diameter. It is filled by sodium without any buffer gas and is heated by a DC-driven coil at each end (the current was switched off during the scans). The cell is placed inside an arrangement of three mutually orthogonal Helmholtz coil pairs in order to compensate stray magnetic fields. However, since the wire of the heating coil is permanent magnetic, it is not possible to compensate the magnetic fields completely for the whole cell volume - a small inhomogeneous field along the laser light propagation was always present. Optimum conditions for the EIT effect are found from measurements of the laser intensity transmitted through the cell at sequential scanning the magnetic fields in all three dimensions, while the difference of the first order frequencies ( $2f_g$ ) is fixed at 1772 MHz. An example of such a scan is shown in Figure 5. Corresponding to the discussion about the influence of the transversal magnetic field (see Fig. 3), maximum transmission at two-photon resonance corresponds to the minimum magnetic field.

Figure 6 represents typical measurements of the transmission signal in dependence on the frequency difference

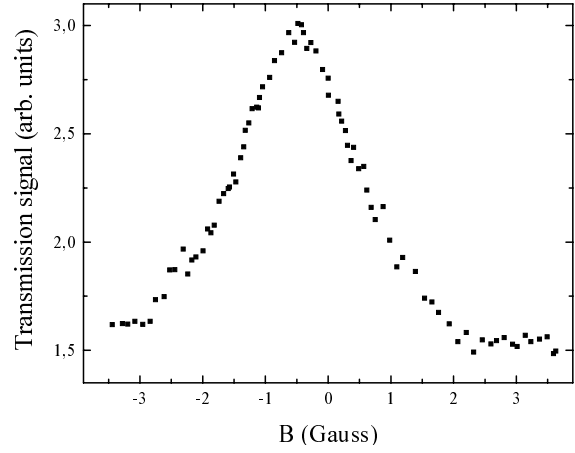


**Fig. 5.** Dependence of the transmitted light intensity on the magnetic field applied in the direction of the laser wave propagation ( $x$ -axis) at fixed magnetic fields in other directions and laser frequency difference ( $\omega_1 - \omega_2$ ) = 1772 MHz. Total laser intensity  $I = 200$  mW/cm<sup>2</sup>. Temperature of the cell 119 °C.

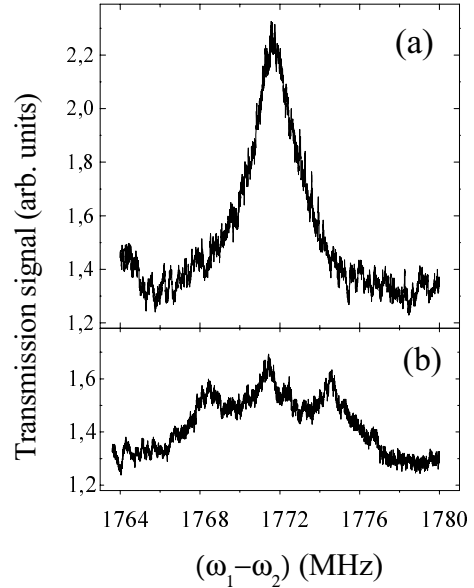


**Fig. 6.** Dependence of the transmitted light intensity on the laser frequency difference ( $\omega_1 - \omega_2$ ). Total laser intensity  $I = 200$  mW/cm<sup>2</sup>. Temperature of the cell  $T = 119$  °C. (a) Magnetic field is maximally compensated in all directions. (b) A magnetic field of 2.14 G is applied in the direction of the laser wave propagation ( $x$ -axis).

( $\omega_1 - \omega_2$ ). The case of maximally compensated magnetic field is shown in Figure 6a. The reduction of light absorption at the two-photon resonance is clearly visible. The halfwidth  $\delta_{\text{EIT}}$  of the intensity peak (transparency window) is smaller than the natural width  $\gamma$  of the excited state  $3^2P_{1/2}$  ( $\gamma = 10$  MHz). This fact indicates that the EIT effect observed in our experiment is really due to quantum interference in CPT, not due to the ac-Stark-shift effect. We have measured the dependence of  $\delta_{\text{EIT}}$  on the input laser intensity (Fig. 7a). As expected, the width  $\delta_{\text{EIT}}$  linearly decreases with decreasing intensity. The

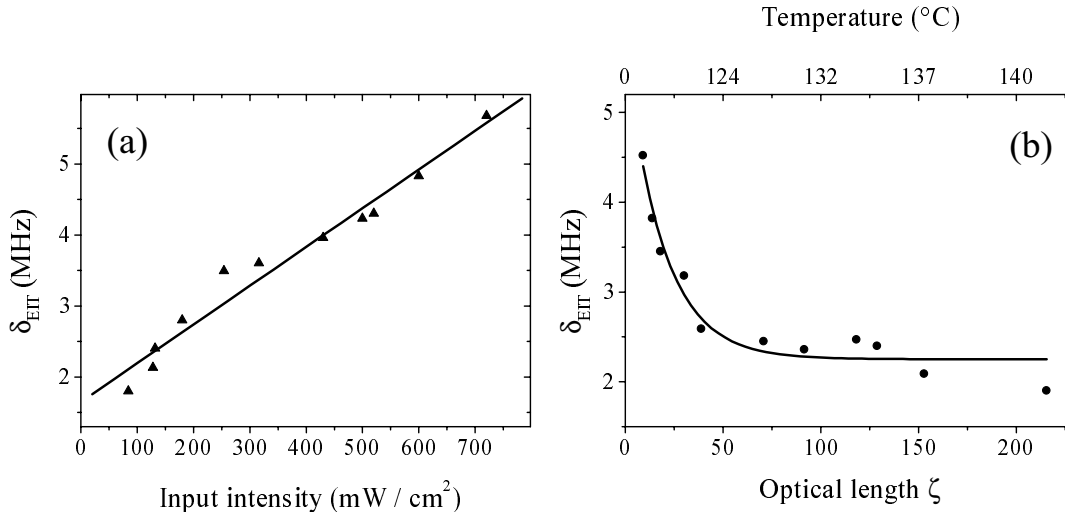


**Fig. 7.** (a) Dependence of the width of the transparency window  $\delta_{\text{EIT}}$  on the total laser intensity at fixed temperature  $T = 129$  °C.  $\blacktriangle$  - experimental points, solid curve - corresponding linear fit. (b) Dependence of  $\delta_{\text{EIT}}$  on the optical length  $\zeta$  - bottom axis (temperature  $T$  - top axis) at fixed total laser intensity  $I = 280$  mW/cm<sup>2</sup>.  $\bullet$  - experimental points, solid curve - exponential decay fit.

minimum intensity necessary for the establishment of CPT - the coherent saturation intensity  $I_c$  [9, 16] - is quite high in our experiment due to the residual magnetic field along the cell and not perfectly eliminated central laser mode (2–4% of the intensity of the sideband modes). We stress that the laser bandwidth has no influence on  $\delta_{\text{EIT}}$  and  $I_c$  since both frequencies are derived from one laser source by use of an EOM, and their phase and amplitude fluctuations are completely correlated. Therefore, in principle, the transparency window can be extremely narrow in this type of EIT experiments - below few tens of Hz [18].

Another series of transmitted intensity scans is taken at different temperatures of the cell. Increase of the temperature leads to an increase of the saturated sodium vapour density  $N$ , and corresponds therefore to the increase of the optical length  $\zeta = (3\pi c^2 N / 4\omega_1^2) x$  for the light transmission. For example, the temperatures  $T = 120$  and  $130$  °C correspond to the length  $\zeta = 36$  and  $84$ , respectively, for our experimental parameters. We observed the behaviour qualitatively in good agreement with theoretical considerations above (Fig. 3) based on the four-level model Figure 1b. The transmitted intensity at two-photon resonance decreases with the temperature (optical length), and the transparency window  $\delta_{\text{EIT}}$  decreases exponentially with the optical length  $\zeta$  (Fig. 7b). We note, however, that in our experiment the light intensity decays faster than expected from the calculations based on the four-level model. The reason is that in the real sodium excitation scheme, except for the  $\Lambda$  systems  $F = 1 \longleftrightarrow F' = 2 \longleftrightarrow F = 2 (m_F = \pm 1)$  and the sink state  $F = 2, m_F = 0$ , there are three two-level systems  $F = 1 \longleftrightarrow F' = 2 (m_F = 0)$  and  $F = 2 \longleftrightarrow F' = 2 (m_F = \pm 2)$  (Fig. 2). The light excites these two-level systems and is absorbed. If stray magnetic fields were zero than the two-level systems populations were quickly pumped into the dark states of the  $\Lambda$  systems and the

state  $F = 2, m_F = 0$ , giving a small additional absorption. However, even a small magnetic field present in our experimental arrangement couples the dark states to the two-level systems. This leads to fairly large absorption not accounted for by the four-level theory.

We have also recorded the transmitted intensity *versus* laser frequency difference ( $\omega_1 - \omega_2$ ) for the cases of an additional magnetic field applied parallel or perpendicular to the laser polarization. The magnetic field parallel to the laser polarization shifts the Zeeman sublevels in energy, and we observe two peaks of transmitted intensity corresponding to two separate  $\Lambda$  systems (with  $m_F = -1$  and  $m_F = +1$ ) with different ground level splittings present for  $\pi$  excitation. Appearance of the three peaks for the perpendicular magnetic field (Fig. 6b) can be explained if we choose the quantization axis parallel to the magnetic field. Then the laser light excites both  $\sigma^+$  and  $\sigma^-$  transitions so that 10 different  $\Lambda$  schemes are formed with three possible ground level splittings [16, 17]. The contrast of each of the peaks is smaller than for the case of compensated magnetic field (Fig. 6a), because the smaller part of atomic population is pumped into corresponding dark states.

### 3 Conclusion

We have investigated the EIT effect in sodium vapour illuminated by two-frequency laser radiation tuned to the D<sub>1</sub> transition. The two frequencies derived from one laser source by use of an EOM have equal polarizations. In this configuration, the EIT effect is due to coherent population trapping in superposition dark states. However, there is an additional optical pumping to states not contributing to the CPT states (external states). We have shown, *via* numerical calculations, that this leads to a smaller contrast of the transparency window as compared to the case of

CPT without losses. A weak magnetic field, which may be present in the experiment, couples the superposition dark state and the external state giving losses out of the CPT state. This leads to further decrease of the contrast and sets a lower limit for the light intensity necessary for the observation of EIT. In our experiment, we have demonstrated the reduction of light absorption for the frequency difference corresponding to the two-photon resonance condition. The width of the transparency window is smaller than the natural width of the excited state in a wide range of the interaction parameters. This fact confirms that the EIT effect is based on a quantum interference effect. We have measured the transparency window  $\delta_{\text{EIT}}$  in dependence on the laser intensity and the temperature of the sodium vapour. It is found that  $\delta_{\text{EIT}}$  increases proportionally to the laser intensity, as it should be in CPT, while it decreases exponentially with increasing temperature (optical length). We have also demonstrated that the transparency window can be splitted into two or three windows by application of an external magnetic field parallel or perpendicular to the light polarization, respectively. The distance between the windows is proportional to the magnitude of the magnetic field strength. Thus, one can change properties of EIT in a quite wide range by changing laser intensity and temperature of the gas, and by application of an magnetic field.

S. B. thanks the members of the Institut für Experimentalphysik, TU Graz, for hospitality and support. This work was supported by the Austrian Science Foundation under project No. S 6508.

## References

1. S.E. Harris, Phys. Today 36 (July 1997).
2. M.O. Scully, Phys. Rep. **219**, 191 (1992).
3. M.O. Scully, M. Fleischhauer, Phys. Rev. Lett. **69**, 1360 (1992).

4. O. Kocharovskaya, Ya.I. Khanin, JETP Lett. **48**, 630 (1988); S.E. Harris, Phys. Rev. Lett. **63**, 1033 (1989); A.S. Zibrov *et al.*, Phys. Rev. Lett. **75**, 1499 (1995); G.G. Padmabandu *et al.*, Phys. Rev. Lett. **76**, 2053 (1996).
5. S.E. Harris, J.E. Field, A. Imamoglu, Phys. Rev. Lett. **64**, 1107 (1990); P.R. Hemmer *et al.*, Opt. Lett. **20**, 982 (1995); S. Babin, U. Hinze, E. Tiemann, B. Wellegehausen, Opt. Lett. **21**, 1186 (1996); A. Apolonskii, S. Balushev, U. Hinze, E. Tiemann, B. Wellegehausen, Appl. Phys. B **64**, 435 (1997).
6. M. Fleischhauer, Phys. Rev. Lett. **72**, 989 (1994).
7. H. Ritsch, M.A.M. Marte, P. Zoller, Europhys. Lett. **19**, 7 (1992); K.M. Gheri, D.F. Walls, Phys. Rev. Lett. **68**, 3428 (1992).
8. For a review of coherent population trapping phenomenon see: B.D. Agap'ev, M.B. Gornyi, B.G. Matisov, Yu.V. Rozhdestvensky, Phys. Uspekhi **36**, 763 (1993); E. Arimondo, in *Progress in Optics*, edited by E. Wolf (Elsevier, Amsterdam, 1996), vol. 35, p.257.
9. M.B. Gornyi, B.G. Matisov, Yu.V. Rozhdestvensky, Zh. Eksp. Teor. Fiz. **95**, 1263 (1989) [Sov. Phys. JETP **68**, 728 (1989)].
10. Y-q. Li, M. Xiao, Phys. Rev. A **51**, R2703 (1995).
11. H.Y. Ling, Y.-Q. Li, M. Xiao, Phys. Rev. A **53**, 1014 (1996).
12. D.E. Nikonov, U.W. Rathe, M.O. Scully, S-Y. Zhu, E.S. Fry, X. Li, G.G. Padmabandu, M. Fleischhauer, Quantum Opt. **6**, 245 (1994).
13. E.A. Korsunsky, W. Maichen, L. Windholz, Phys. Rev. A **56**, 3908 (1997).
14. M.O. Scully, M.S. Zubairy, *Quantum Optics* (Cambridge University Press, Cambridge, 1997).
15. I.I. Sobelman, *Atomic spectra and radiative transitions* (Springer-Verlag, Berlin, 1979), p. 198.
16. A.M. Akulshin, A.A. Celikov, V.L. Velichansky, Opt. Commun. **84**, 139 (1991).
17. O. Schmidt, R. Wynands, Z. Hussein, D. Meschede, Phys. Rev. A **53**, R27 (1996).
18. S. Brandt, A. Nagel, R. Wynands, D. Meschede, Phys. Rev. A **56**, R1063 (1997).